*J. Physiol.* (1978), **276**, *pp.* 67–82
*With 8 text-figures*
*Printed in Great Britain*



# THE DEPENDENCE OF MEMBRANE POTENTIAL ON EXTRACELLULAR CHLORIDE CONCENTRATION IN MAMMALIAN SKELETAL MUSCLE FIBRES

BY ANGELA F. DULHUNTY

*From the Department of Anatomy, University of Sydney, N.S.W., Australia*

(*Received 14 July 1977*)

SUMMARY

1. The steady-state intracellular membrane potential of fibres in thin bundles dissected from mouse *extensor digitorum longus* or *soleus* muscles or rat *sternomastoid* muscles was measured with 3 M-KCl glass micro-electrodes. The steady-state membrane potential was found to depend on the extracellular concentrations of Na, K and Cl ions.

2. The resting membrane potential (3·5 mM-$[K]_o$, 160 mM-$[Cl]_o$) was $-74 \pm 1$ mV (mean $\pm$ S.E.) and a reduction in $[Cl]_o$ to 3·5 mM caused a reversible steady-state hyperpolarization to $-94 \pm 1$ mV (mean $\pm$ S.E.).

3. The steady-state membrane potentials recorded in fibres exposed to different $[K]_o$ and zero $[Cl]_o$ were consistent with potentials predicted by the Goldman, Hodgkin & Katz (GHK) equation for Na and K. The results of similar experiments done with Cl as the major external anion could not be fitted by the same equation.

4. The GHK equation for Na, K and Cl did fit data obtained from fibres in solutions containing different $[K]_o$ with Cl as the major external anion if the intracellular Cl concentration was allowed to be out of equilibrium with the steady-state membrane potential.

5. It is suggested that an active influx of Cl ions controls the intracellular Cl concentrations in these fibres and hence maintains the Cl equilibrium potential at a depolarized value with respect to the resting membrane potential.

6. The steady-state membrane potential of rat diaphragm fibres was independent of $[Cl]_o$ and it seems likely that the intracellular Cl concentration of these fibres is not controlled by active Cl transport.

## INTRODUCTION

The steady-state membrane potential, $V_m$, of mammalian skeletal muscle fibres is less sensitive to changes in external K concentration, $[K]_o$, than $V_m$ of amphibian skeletal muscle fibres when $[K]_o$ is altered over the same range of concentrations (Dulhunty, 1977*a*). Hodgkin & Horowicz (1959, 1960) found that $V_m$ in single amphibian muscle fibres could be simply predicted by the Goldman, Hodgkin and Katz (GHK) equation for Na and K, i.e.

$$V_m = \frac{RT}{F} \ln \frac{[K]_o + \alpha[Na]_o}{[K]_i + \alpha[Na]_i} \quad (1)$$

where $R$, $T$ and $F$ have their usual meaning, $\alpha$ is the ratio of Na permeability to K permeability ($P_{Na}/P_K$) and subscripts i and o refer to the concentration of ions inside and outside the fibres. The distribution of Na and K ions is similar in amphibian and mammalian preparations (Lipicky & Bryant, 1966) and, if $\alpha$ is not significantly different, eqn. (1) predicts the same $V_m$. The resting membrane potential of mammalian fibres (inside with respect to outside) is however 15–40 mV less negative (Boyd & Martin, 1959; Bryant, 1969; Luff & Atwood, 1972) than that of amphibian fibres (see e.g. Hodgkin & Horowicz, 1960), implying that either $\alpha$ is different or additional ions contribute to $V_m$ in mammalian fibres. In the second case the internal concentration of the ion would have to be set by an active transport process and the membrane permeability to the ion would have to be high. An obvious possibility is that Cl ions are important since mammalian fibres have been shown to have a high Cl permeability (Lipicky & Bryant, 1966; Palade & Barchi, 1977).

The experiments described in this paper show that membrane potential in mammalian fibres depends on external Cl concentration and that the contribution of Cl is sufficient to explain the deviation from related amphibian results.

Preliminary reports of some of these results have appeared elsewhere (Dulhunty, 1977*b*).

## METHODS

The preparations used were the *sternomastoid* muscle of adult male Wistar rats and the *extensor digitorum longus* (EDL) and *soleus* muscles from adult male or female C57BL mice (the mice are a Bar Harbor strain bred in the laboratory). Measurements were made on surface fibres of bundles two or three fibres thick and up to forty fibres across. The rat sternomastoid muscle was most commonly used because it is more suited to fine dissection and because the fibres are grouped into bundles of red and white fibres which can be separated under the dissecting microscope. The cross-sectional areas of 117 red fibres and seventy-one white fibres measured from frozen sections were $2356 \pm 111$ $\mu m^2$ and $3865 \pm 130$ $\mu m^2$ (means $\pm$ S.E.) respectively. The preparations were mounted on Sylgard (Dow Corning) in a narrow Perspex bath containing Krebs solution (see below). The centre part of the bundle passed over a raised Perspex bridge so that micro-electrodes could be inserted more easily. The preparations were maintained at $37 \pm 1$ °C.

*Solutions.* The solutions commonly used are listed in Table 1. The normal solution contained either $HPO_4/HCO_3$ buffer (solution D) or HEPES buffer (solution A) at pH = 7·4. Similar electrophysiological results were obtained with the two buffers and most experiments were done using HEPES (solutions A, B, and C) since the solutions were more stable. Tetrodotoxin ($10^{-7}$ g/ml.) was added to solutions to prevent action potentials and twitches. All solutions were bubbled with 95 % $O_2$ and 5 % $CO_2$. The solutions flowed continuously over the preparation and the solution in the bath could be changed completely in 2 sec at maximum flow rates.

*Electrophysiology.* Intracellular membrane potentials were measured with glass micro-electrodes filled with 3 M-KCl (resistance 2–20 MΩ). The bath electrode was either a salt bridge made with 3 M-KCl in agar, or a second micro-electrode (see e.g. Hodgkin & Horowicz, 1959). Records were obtained on chart paper using a Hewlett Packard (7402A) pen recorder.

*Junction potential considerations.* An inherent error in the measurement of intracellular membrane potential comes from the junction potential between the electrode solution (3 M-KCl) and the solution outside the electrode. A change in junction potential following a change in the ionic composition of the experimental solution could be misinterpreted as a change in membrane potential. The difference between junction potentials calculated for control and test solutions (Tables 1 and 2), using equations given by Barry & Diamond (1970), was less than 1 mV in all cases except the sulphate solutions where the greatest difference was +3·1 mV in $MgSO_4$ (Table 2; 1717). The calculated changes were never more than 10 % of the measured change in $V_m$ in a particular solution.

TABLE 1. Solutions

| Solution | Na | K | Ca | Cl | $NO_3$ | $SO_4$ | $PO_4$ | $HCO_3$ | HEPES | Sucrose | Ionic strength | Osmolarity |
|---|---|---|---|---|---|---|---|---|---|---|---|---|
| A | 150 | 3·5 | 2·5 | 160·5 | — | — | — | — | 1·0 | — | 165·0 | 330·5 |
| B | 84 | 3·5 | 6·0 | — | — | 50·75 | — | — | 1·0 | 169·25 | 160·0 | 328·5 |
| C | 0 | 150·0 | 2·5 | 157·0 | — | — | — | — | 1·0 | — | 161·5 | 324·5 |
| D | 145 | 3·5 | 2·5 | 128·5 | — | — | 3·0 | 25 | — | — | 171·5 | 320·5 |
| E | 204 | 3·5 | 2·5 | 186·5 | — | — | 3·0 | 25 | — | — | 230·0 | 437·5 |
| F | 204 | 3·5 | 2·5 | — | 186·5 | — | 3·0 | 25 | — | — | 230·0 | 437·5 |
| G | 132 | 3·5 | 6·0 | — | — | 59·75 | 3·0 | 25 | — | 195·25 | 227·25 | 437·5 |
| H | 28 | 180·0 | 2·5 | 187 | — | — | 3·0 | 25 | — | — | 230·5 | 438·5 |
| I | 28 | 200·0 | 2·5 | — | 205·0 | — | 3·0 | 25 | — | — | 240·5 | 476·5 |
| J | 28 | 180·0 | 6·0 | — | — | 96·0 | 3·0 | 25 | — | 129·0 | 336·0 | 480·0 |
| K | 28 | 200·0 | 2·5 | 205 | — | — | 3·0 | 25 | — | — | 249·5 | 476·5 |
| L | 28 | 220·0 | 2·5 | 225 | — | — | 3·0 | 25 | — | — | 269·5 | 516·5 |

Osmolarity in m-osmole. Ion concentrations in mM. In addition all solutions contained 1 mM-Mg and 12 mM-glucose.

## RESULTS

### *Resting membrane potential*

The membrane potential recorded from fibres in normal Krebs solution (solution A or D; Table 1) varied considerably from one preparation to the next although fibres within a preparation had similar potentials. When two muscles were taken from the same animal they frequently had similar average resting potentials (see Table 2A). The average potentials varied over 19 mV from −62 (1127) to −81 mV (717), although the greatest difference between the two muscles from one animal was only 5·6 mV (227). The results from all experiments, including those listed in

TABLE 2. (A) Membrane potentials of two muscles dissected from one animal (mean ± S.E.)

| Mouse | | | Rat | | |
|---|---|---|---|---|---|
| | Membrane potential (mV) | | | Membrane potential (mV) | |
| Code | EDL | Soleus | Code | White sterno-mastoid | Red sterno-mastoid |
| 2617 | −70·0 ± 3·5 | −75·5 ± 2·8 | 1717 | −77·0 ± 2·5 | −73·0 ± 2·5 |
| 227 | −78·3 ± 1·9 | −72·7 ± 2·6 | 1427 | −69·0 ± 2·3 | −71·0 ± 4·0 |
| 1127 | −67.3 ± 1·3 | −61·9 ± 2·3 | 617 | −74·0 ± 2·5 | −76·7 ± 3·0 |
| 2327 | −71·8 ± 1·3 | −69·1 ± 1·8 | 717 | −80·0 ± 2·3 | −80·6 ± 1·8 |

(B) Range of membrane potentials recorded from different mammalian preparations and pooled results from all fibres (mean ± S.E.). Figures in parenthesis give the total number of fibres measured

| Muscle | Range: Lowest average potential (mV) | Range: Highest average potential (mV) | Average potential (mV) |
|---|---|---|---|
| Mouse EDL | −61·2 ± 1·9 | −79·7 ± 2·6 | −71·5 ± 0·9 (78) |
| Mouse soleus | −62·0 ± 1·1 | −75·5 ± 2·7 | −70·0 ± 0·9 (75) |
| Rat red SM | −61·3 ± 1·0 | −81·7 ± 0·8 | −70·7 ± 0·6 (223) |
| Rat white SM | −64·5 ± 1·7 | −82·4 ± 1·6 | −72·4 ± 0·8 (104) |

Table 2A, are summarized in Table 2B. The highest and lowest average potentials from individual preparations are given and the average of all fibres is listed in the last column with the total number in brackets. The pooled results for the different muscles are remarkably similar and there is not a significant difference among the four muscles examined.

The following results have not been grouped according to the type of muscle used, since the responses of the four muscles to changes in external ion concentrations were similar.

*Ions influencing the resting membrane potential.* Changing the external concentration of an ion that contributes to the membrane potential should alter the steady-state membrane potential by an amount that depends on the internal and external concentrations of the ion and the relative membrane permeability to the ion. The

TABLE 3. Effect of ion substitution on membrane potential (the number of fibres, $n$, is given in parentheses in the last column)

| Prep. | Ion excluded | Na (mM) | Na substitute (S) | S (mM) | Anion (A) | A (mM) | Buffer* | Sucrose (mM) | Ionic strength | Osmolality (m-osmole) | $V_m \pm$ S.E. (mV) | ($n$) |
|---|---|---|---|---|---|---|---|---|---|---|---|---|
| 1736 | — | 145 | — | — | Cl | 128·5 | $HPO_4/HCO_3$ | — | 159·5 | 320·5 | −67·3 ± 0·6 | (15) |
| | $HCO_3$† | 145 | — | — | Cl | 128·5 | $PO_4$ | — | 159·5 | 320·5 | −68·0 ± 0·1 | (14) |
| 1717 | — | 145 | — | — | Cl | 128·5 | $HPO_4/HCO_3$ | — | 159·5 | 320·5 | −77·0 ± 2·5 | (10) |
| | $HCO_2$, $HPO_4$ | 150 | — | — | Cl | 160·5 | HEPES | — | 165·0 | 329·5 | −78·5 ± 1·7 | (10) |
| 656 | — | 204 | — | — | Cl | 186·5 | $HPO_4/HCO_3$ | — | 218·0 | 437·5 | −72·8 ± 1·8 | (20) |
| | Cl | 204 | — | — | $NO_3$ | 186·5 | $HPO_4/HCO_3$ | — | 218·0 | 437·5 | −76·0 ± 0·8 | (12) |
| 866 | — | 204 | — | — | Cl | 186·5 | $HPO_4/HCO_3$ | — | 218·0 | 437·0 | −69·3 ± 0·7 | (16) |
| | Cl | 132·0 | — | — | $SO_4$ | 59·75 | $HPO_4/HCO_3$ | 195·25 | 215·25 | 436·5 | −83·7 ± 2·2 | (10) |
| 237 | — | 150·0 | — | — | Cl | 160·5 | HEPES | — | 165·0 | 329·5 | −76·8 ± 4·6 | (8) |
| | Cl | 84·0 | — | — | $SO_4$ | 50·75 | HEPES | 169·25 | 161·5 | 328·5 | −98·1 ± 3·8 | (15) |
| 18126 | — | 150 | — | — | Cl | 160·5 | HEPES | — | 165·0 | 329·5 | −65 ± 1·3 | (10) |
| | Na† | — | Choline | 150 | Cl | 160·5 | HEPES | — | 160·25 | 329·5 | −60·2 ± 1·8 | (5) |
| 1866 | — | 84 | — | — | $SO_4$ | 50·75 | HEPES | 169·25 | 161·5 | 328·5 | −86·8 ± 1·0 | (9) |
| | Na† | 42 | Sucrose | 63 | $SO_4$ | 29·5 | HEPES | 169·25 | 96·27 | 328·25 | −70·6 ± 1·3 | (5) |
| | Na† | — | Sucrose | 126 | $SO_4$ | 8·75 | HEPES | 169·25 | 34·25 | 328·5 | −61·8 ± 0·3 | (5) |
| 1717 | — | 150 | — | — | Cl | 160·5 | HEPES | — | 165·0 | 329·5 | −77·0 ± 1·8 | (10) |
| | Na† | 0 | Mg | 75 | Cl | 160·5 | HEPES | 73·0 | 238·0 | 329·5 | −83·4 ± 1·9 | (10) |
| | Na, Cl† | 0 | Mg | 75 | $SO_4$ | 82·75 | HEPES | 148·25 | 330·25 | 329·5 | −44·0 ± 3·6 | (10) |

In addition all solutions contained 3·5 mM-K, 1 mM-Mg, and 12 mM-glucose. Cl solutions contained 2·5 mM-Ca and $SO_4$ solutions contained 6·0 mM-Ca.

* $HPO_4/HCO_3$ buffer was made with 3·0 mM-$HPO_4$ and 25 mM-$HCO_3$. HEPES buffer was 1 mM.

† Solutions that were only used for the experiment shown and are not listed in Table 1 with the commonly used solutions.

results of initial experiments to observe the effect of removing ions normally present in the external solution are given in Table 3. The results of changing K concentration have not been included at this stage. The steady-state membrane potential was measured in control solution before and after exposure to the test solution, and the average of these measurements is given in Table 3 as well as the average potential measured after 30 min in the test solution. The potential was not altered by removal of $HPO_4$ or $HCO_3$ in the first two experiments (1736, 1717). Replacement of Cl with $SO_4$ was followed by hyperpolarizations of 14·4 mV in preparation 866 and 23·3 mV in preparation 237. Replacement of Cl with $NO_3$ was followed by a 3·2 mV hyperpolarization (656). The results for 866 and 237 show that the normal resting potential is hyperpolarized when $[Cl]_o$ is lowered. The less significant hyperpolarization with $NO_3$ substitution suggests that $NO_3$ may partially replace Cl in its effect on the steady-state potential.

The effect of Na removal is shown in the last three preparations in Table 3. Replacement of Na by Mg (1717) caused a 6·4 mV hyperpolarization which is consistent with a GHK equation containing a Na term (see eqn. (1) and eqn. (2) below) and a relatively low resting permeability to Na. When Cl was also removed (1717) a reversible 33 mV depolarization was recorded. Replacement of Na with choline or sucrose (18126, 1866) also caused a depolarization which was greater in the absence of Cl (1866). A depolarization in low Na solutions is not simply predicted by the GHK equation but is consistent with previous observations on the effects of external cations on membrane potential in frog semitendinosus fibres (Dulhunty & Horowicz, 1975), i.e. that K permeability depends on the valency and total concentration of cations.

Experiments were done to investigate the dependence of membrane potential on the external Cl concentration since significant changes in membrane potential were seen when $[Cl]_o$ was replaced by $SO_4$.

*Dependence of membrane potential on external Cl.* Cl concentration in the solution was varied by mixing different proportions of solutions A and B (Table 1). $[Na]_o$ was lowered to 84 mM in solution B to maintain ionic strength. However, it will be shown that the effect of changing from solution A (150 mM-$[Na]_o$, 160 mM-$[Cl]_o$) to solution B (84 mM-$[Na]_o$, 0 mM-$[Cl]_o$) is significantly different from the effect of simply reducing $[Na]_o$ from 150 to 84 mM in either Cl-containing or Cl-free solutions. One record obtained when $[Cl]_o$ was lowered from 160 to 80 mM is shown in Fig. 1. A transient 5 mV depolarization was recorded as soon as external Cl was reduced. Then the membrane potential started to become more negative until it was 14 mV more hyperpolarized than originally. Conversely, when $[Cl]_o$ was restored to its normal concentration, an initial hyperpolarization preceded the return of the membrane potential to its original value.

The steady-state potential after 6–8 min in the low Cl solution (Fig. 1) depended on the concentration of Cl in the solution as shown in Fig. 2, and the membrane potential in 3·5 mM-$[Cl]_o$ was 20·8 mV more hyperpolarized than in 160 mM-$[Cl]_o$. However, the mechanism responsible for this result is not immediately apparent. In separate experiments it was found that lowering $[Na]_o$ from 150 to 84 mM caused hyperpolarizations of less than 3 mV with Cl as the major external anion. Reducing $[Na]_o$ from 150 to 84 mM in $SO_4$ solutions caused either a small hyperpolarization

or a small depolarization, both of which were less than 2 mV. It is therefore unlikely that the results shown in Figs. 1 and 2 could be explained by the reduced $[Na]_o$; the hyperpolarization must be caused by the reduced $[Cl]_o$. External Cl could influence $V_m$ by modifying the conductances of ions contributing to the membrane potential. A simpler hypothesis is that Cl contributes to the membrane potential and $V_m$ follows a GHK equation for Na, K and Cl of the form:

$$V_m = \frac{RT}{F} \ln \frac{[K]_o + \alpha[Na]_o + \gamma[Cl]_i}{[K]_i + \alpha[Na]_i + \gamma[Cl]_o} \quad (2)$$

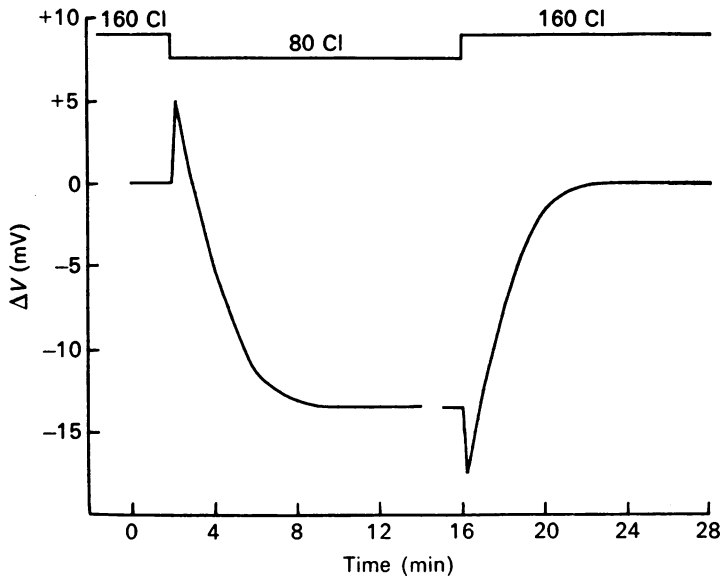


Fig. 1. Membrane potential, $\Delta V_m$ in mV, from a red sternomastoid fibre exposed to 80 mM-$[Cl]_o$ (80 Cl) for 10 min has been redrawn from the original record. The horizontal axis shows time in min and zero time is at the time of penetration of the fibre. The duration of exposure to 80 mM-$[Cl]_o$ is indicated along the top of the diagram. The resting membrane potential was −74 mV in 160 mM-$[Cl]_o$. Zero membrane potential on the vertical axis is the resting potential in 160 mM-$[Cl]_o$ and hyperpolarization is downward.

(where $R$, $T$, $F$, $\alpha$, i and o have been defined previously, and $\gamma = P_{Cl}/P_K$). Other ions have not been included in the equation since there is no evidence for a significant permeability to other ions normally present in high enough concentrations to influence $V_m$. A steady-state hyperpolarization in low Cl solutions could follow a reduction of $P_{Cl}/P_K$ or a reduction in $[Cl]_i$. The results in Fig. 1 suggest that $P_{Cl}/P_K$ does not fall significantly in the low Cl solution. The mechanism altering the steady-state potential is not instantaneously dependent on $[Cl]_o$ since the membrane potential takes 6–8 min to stabilize after a change in Cl concentration. The transient potential changes therefore follow the change in $[Cl]_o$. If $P_{Cl}/P_K$ fell to a very low value during exposure to low $[Cl]_o$, the membrane potential should be relatively insensitive to further changes in $[Cl]_o$. The 'off' transient shown in Fig. 1 means that membrane potential is still sensitive to changes in $[Cl]_o$. If $P_{Cl}/P_K$ is not significantly

altered in low $[Cl]_o$, the steady-state hyperpolarization shown in Figs. 1 and 2 must be caused by a reduction in the internal Cl concentration and the time taken for $V_m$ to reach a steady-state value after changes in $[Cl]_o$ is a reflexion of the time taken for the internal Cl concentration to change. Internal Cl concentrations have been calculated for the different $[Cl]_o$, assuming that $P_{Cl}/P_K$ is constant, and are shown in Fig. 3 (constants used in the calculation are given in the figure legend).

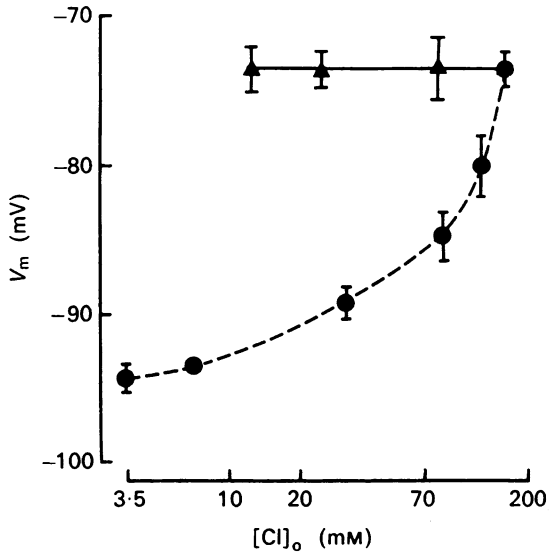


Fig. 2. Steady-state membrane potential, $V_m$ in mV, recorded after 10 min in solutions containing Cl concentrations shown in mM on the horizontal axis. The solutions are appropriate combinations of solutions A and B listed in Table 1. The filled circles are the mean of membrane potentials from rat sternomastoid and mouse EDL and soleus preparations. The vertical bars indicate ± 1 S.E. The line through the point has been drawn by eye. The triangles are the mean of membrane potentials recorded from one rat diaphragm preparation and the vertical bars indicate ± S.E. Each set of measurements in $[Cl]_o$ less than 160 mM was bracketed by measurements in 160 mM-$[Cl]_o$. The membrane potential shown for 160 mM-$[Cl]_o$ is therefore the average of control membrane potentials throughout the experiment.

The results in Figs. 1 and 2 show conclusively that membrane potential depends on external Cl concentration. The results do not however give information about how $[Cl]_o$ influences membrane potential. The data can be fitted by the GHK equation for Na, K and Cl, and the following experiments have been done to see whether the relation between external K and membrane potential in Cl solutions is consistent with the same equation.

### *Membrane potential in different* $[K]_o$

*Time course of depolarization after raising* $[K]_o$. It was necessary to look at the time course of depolarization following an increase in $[K]_o$ from its normal concentration of 3·5 mM to determine the time taken to reach a steady-state potential. Membrane potential was recorded by multiple penetration of fibres in a preparation exposed to 65 mM-$[K]_o$ (solution A + solution C; Table 1) for 3·5 hr (see Fig. 4*A*). $[Cl]_o$ was constant and the $[K]_o \times [Cl]_o$ product increased with $[K]_o$. The membrane

potential of amphibian skeletal muscle fibres exposed to solutions with a high $[K]_o \times [Cl]_o$ product can take up to 1 hr to reach a steady-state value because of slow changes in internal Cl concentrations (Hodgkin & Horowicz, 1959). In Fig. 4*A* the membrane potential reached its steady-state value between 4 and 5 min and the average potential of four fibres between 5 and 10 min was $-30{\cdot}75 \pm 1{\cdot}1$ mV and of eight fibres, between 3·3 and 3·5 hr, was $-31 \pm 0{\cdot}84$ mV (means ± S.E.). The time course of recovery, illustrated in Fig. 4*B*, is similar after 5 min (dashed line) and 3·5 hr exposure (filled circles) suggesting that the slow ion redistribution, characteristic of amphibian muscle fibres (Hodgkin & Horowicz, 1959), may not occur in mammalian muscle fibres.

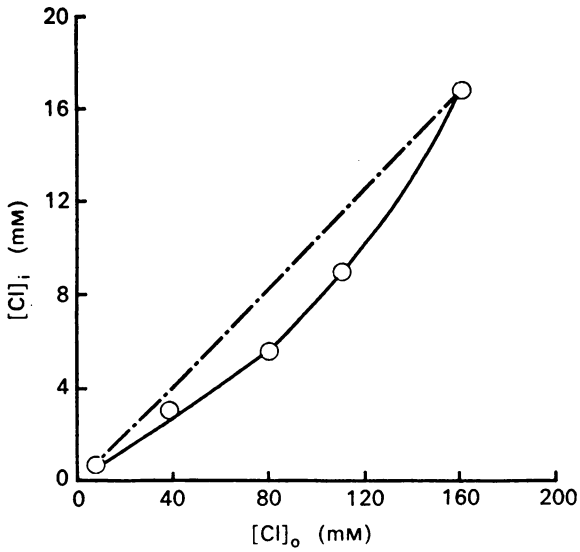


Fig. 3. Internal Cl concentrations, $[Cl]_i$ in mM, calculated for external Cl concentrations, $[Cl]_o$ in mM, shown on the horizontal axis. The internal Cl concentrations were calculated with eqn. (2) using the membrane potentials given in Fig. 2 with the following constants: $[Na]_o$ = 80–150 mM, $[K]_o$ = 3·5 mM (solutions A and B, Table 1), $[Na]_i$ = 60 mM, $[K]_i$ = 157 mM (Lipicky & Bryant, 1966), $\alpha$ = 0·008 (calculated in text for Fig. 8), and $\gamma$ = 1 (see Figs. 7 and 8). The dashed line is a straight line drawn from the origin to the $[Cl]_i$ calculated for the normal $[Cl]_o$ = 160 mM. The continuous line has been drawn through the calculated points by eye.

The initial time course of depolarization was recorded continuously in individual fibres and the result from one fibre exposed to 80 mM-$[K]_o$ in the presence of $[Cl]_o$ is shown in Fig. 5 (open circles, curve *a*). The membrane potential took between 3 and 4 min to reach a constant value. The membrane potential changed more quickly if $[K]_o$ was increased in Cl-free solutions. A continuous record from a red sternomastoid fibre exposed to 60 mM-$[K]_o$ with zero $[Cl]_o$ is also shown in Fig. 5 (open triangles, curve *b*). The steady-state potential was reached between 1 and 2 min.

The time course of initial depolarization shown in Fig. 5 (curves *a* and *b*) is much slower than that reported for amphibian fibres under similar conditions (Hodgkin & Horowicz, 1960). Significant slowing of the potential transients could be the result

of diffusion delays associated with the larger bundles of fibres dissected from mammalian muscles. The possibility of significant diffusion delays was investigated using similar bundles of toad semitendinosus fibres and the time course of depolarization in one fibre exposed to 10 mM-$[K]_o$ is shown in curve *c* (filled circles, continuous curve). Depolarization took about 10 sec but was 80% complete in less than 2 sec. The rate of depolarization was therefore slowed by the use of bundles but not sufficiently to explain the time course shown in curves *a* and *b* (Fig. 5) for mammalian fibres. The time course of initial membrane potential changes in response to sudden increases in external K concentration are therefore considerably slower in mammalian muscle.

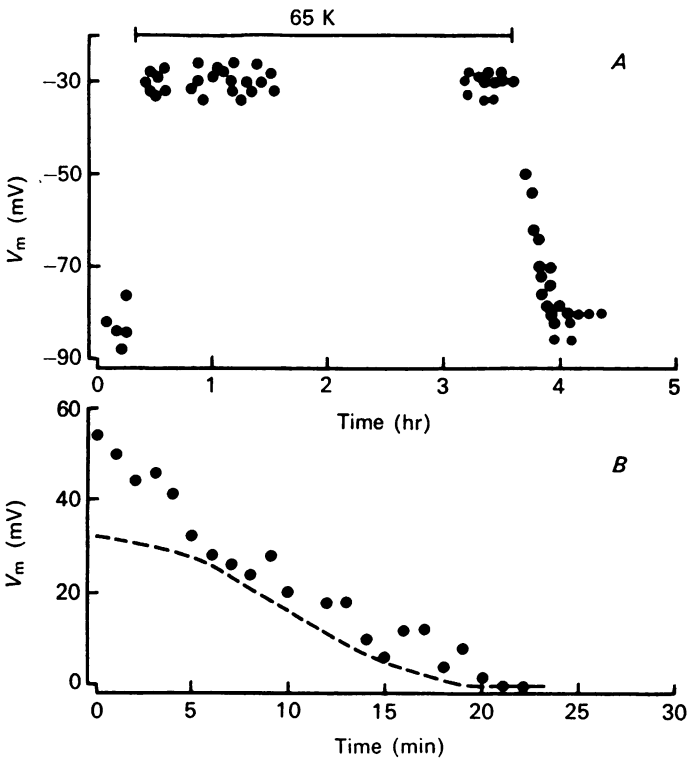


Fig. 4. Membrane potential, $V_m$ in mV, recorded by multiple penetration of one preparation of red sternomastoid fibres exposed to 65 mM-$[K]_o$ for 3·5 hr (solution A and solution C, Table 1). Each dot is the membrane potential recorded from one fibre. *A*: membrane potential is shown before, during and after exposure to 65 mM-$[K]_o$ for the period indicated by the line above the graph. *B*: recovery of membrane potential after long exposure, measured by multiple penetration (filled circles), is shown on an expanded time scale and compared with recovery after a 5 min exposure to 80 mM-$[K]_o$ (solution F and solution H) (dashed line) in a continuous recording experiment.

### *Membrane potential in Cl-free solutions and high* $[K]_o$

Spontaneous contractures were observed for 1–2 hr after preparations were exposed to Cl-free solutions (solutions F or G, Table 1) and records were not taken until this had ceased. The average hyperpolarization in Cl-free solutions was less than in solutions with a low Cl concentration. For example in two preparations

average hyperpolarizations of 4·8 and 9·2 mV were recorded in the Cl-free solution which can be compared with the 20 mV hyperpolarization in 3·5 mM-$[Cl]_o$ (see Fig. 2).

$[K]_o$ was varied by mixing different proportions of either solutions F and I or solutions G and J (Table 1). Fig. 6 shows the steady-state potential as a function of $[K]_o$ when the external anion was $SO_4$ (filled circles) and $NO_3$ (open circles). If $V_m$ is independent of internal Cl in Cl-free solutions and the contribution of other ions is small, membrane potential should be predicted by the GHK equation for Na and

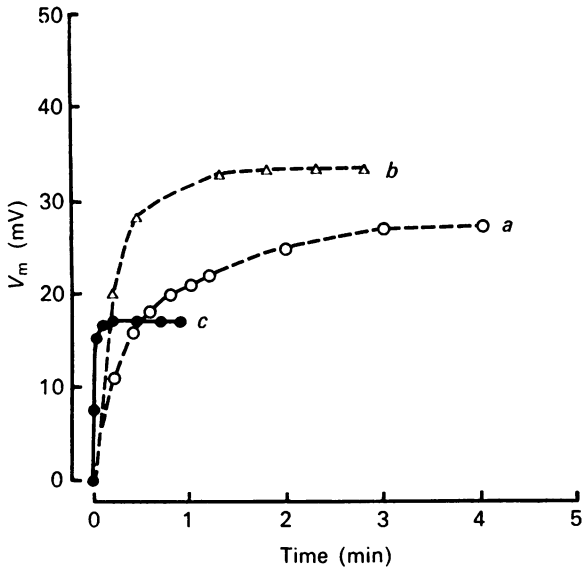


Fig. 5. Membrane potential, $\Delta V_m$ in mV, as a function of time (min) after rapid exposure to high K solutions. The symbols are taken from continuous records from individual fibres during the solution changes. All fibres were on the surface of similar sized bundles. Curve *a* is drawn through the open circles for a red sternomastoid fibre, exposed to 60 mM-$[K]_o$ with Cl as the major external anion (solution E and solution H, Table 1). Curve *b* is drawn through the open triangles for a red sternomastoid fibre exposed to 65 mM-$[K]_o$ with $SO_4$ as the major external anion (solution G and solution J). Curve *c* drawn through the filled circles for a toad semitendinosus fibre exposed to 10 mM-$[K]_o$ with Cl as the major external anion in a conventional amphibian Ringer solution. Mechanical activity was elicited at lower K concentrations in the semitendinosus preparations (Dulhunty, 1977*a*) and continuous records of membrane potential had to be obtained using lower K concentrations.

K (eqn. (1)). The interrupted line in Fig. 6 was calculated with eqn. (1) as described in the Figure legend. The curve is a good fit to the $SO_4$ data and it is reasonable to suppose that membrane potential depends primarily on the Na and K in $SO_4$ solutions. It is interesting to note that equation 1 provides a good fit to the experimental data only if $\alpha = 0{\cdot}03$ is used. This is greater than the value of $\alpha = 0{\cdot}008$ obtained in low Cl (rather than Cl-free) solutions in Fig. 2 and suggests that $P_{Na}/P_K$ changes in Cl-free solutions may be responsible for the relatively low membrane potential in this solution.

*Effect of* $[Cl]_o$ *on the relation between membrane potential and* $[K]_o$

The details of solutions used are given in the legend to Figs. 7 and 8. All solutions used to obtain results in Fig. 7 were hypertonic to allow $[K]_o$ to be increased to 180 mM without a change in the tonicity of the solution. The membrane potential with $[Na]_o$ = 204 mM, $[Cl]_o$ = 187 mM and $[K]_o$ = 3·5 mM was −64 mV. The results shown in Fig. 7 (filled circles) cannot be fitted by the GHK equation for Na and K, i.e. eqn. (1), (continuous line) used in the same way as for Fig. 6. Eqn. (1) could not be made to fit the data even when $\alpha$ and $[K]_i$ were varied over a reasonable

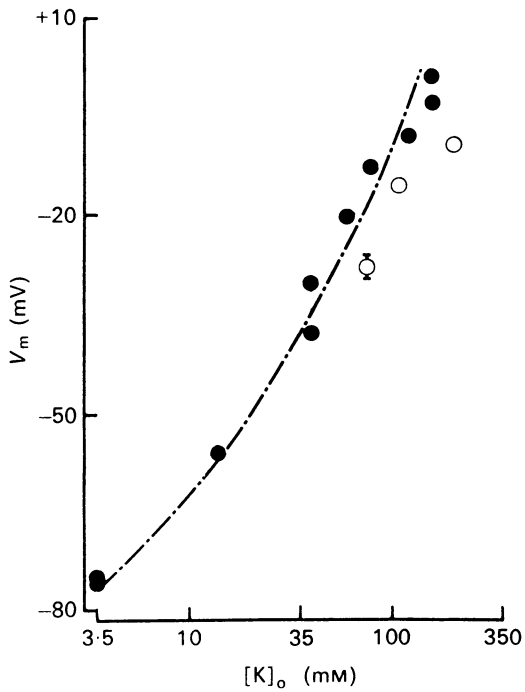


Fig. 6. Membrane potential, $V_m$ in mV, is shown as a function of the logarithm of external K, $[K]_o$ in mM. Symbols are the average steady-state membrane potentials from bundles of red and white sternomastoid fibres in Cl-free solutions. The vertical bars represent ± S.E. where this is greater than the dimension of the symbol. Filled circles: Cl replaced by $SO_4$ (solution G and solution J, Table 1). Open circles: Cl replaced by $NO_3$ (solution F and solution I). The interrupted line was calculated with eqn. (1). $\alpha$ = 0·03 was determined for $V_m$ in 3·5 mM-$[K]_o$ using $[K]_i$ = 157 mM and $[Na]_i$ = 60 mM (Lipicky & Bryant, 1966). $\alpha$, $[Na]_i$ and $[K]_i$ were then assumed to be constant and the $V_m$ calculated for different $[K]_o$ and $[Na]_o$ is shown with the interrupted line.

range (i.e. $\alpha$ = 0–0·1 and $[K]_i$ = 117–200 mM). The dashed line was calculated from the GHK equation for Na, K and Cl (eqn. (2)) using best fit values of $\gamma$ = 1 and $[Cl]_i$ = 27 mM. Equally good fits could be obtained assuming that $[Cl]_i$ could vary. For example least squares analysis with $\gamma$ = 4 (Lipicky & Bryant, 1966; Palade & Barchi, 1977) gave the best results when $[Cl]_i$ increased from 19·6 mM in 3·5 mM-$[K]_o$ to 56 mM in 68 mM-$[K]_o$.

A second set of data obtained from one bundle of red sternomastoid fibres is shown in Fig. 8 (triangles). These results were obtained under isotonic conditions and $[K]_o$ was not increased above 150 mM. The resting membrane potential measured

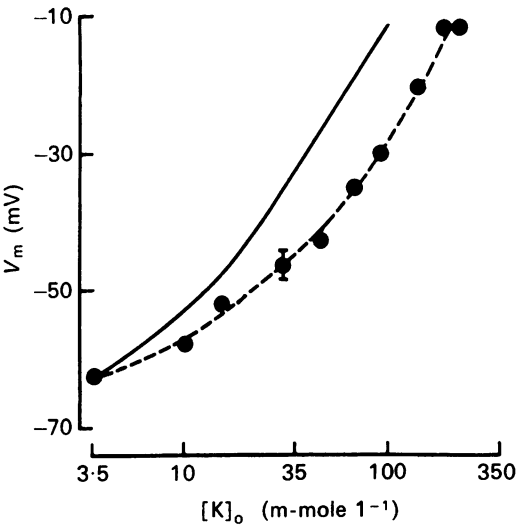


Fig. 7

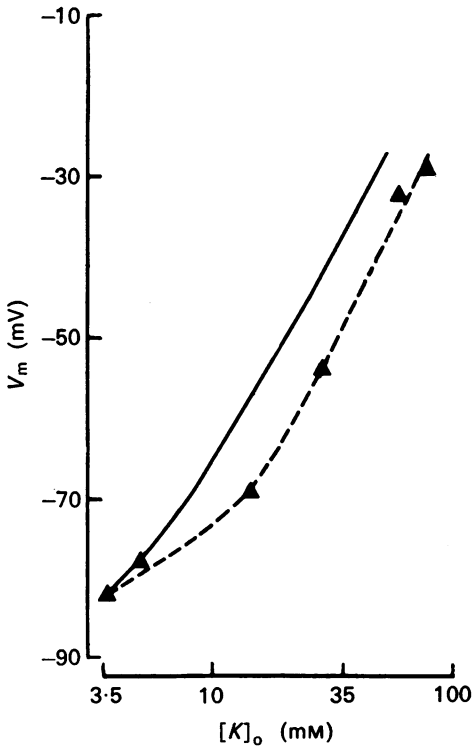


Fig. 8

Fig. 7. Membrane potential, $V_m$ in mV, is shown as a function of the logarithm of external K, $[K]_o$ in mM. Filled circles are the average steady-state membrane potentials from three red and two white sternomastoid bundles exposed to different concentrations of external K up to 180 mM with constant external Cl (solution E and H, Table 1). Solutions were all made hypertonic so that $[K]_o$ could be increased to 180 mM without altering tonicity or ionic strength. For $[K]_o$ greater than 180 mM, Cl concentration, tonicity and ionic strength were increased (solutions K and L, Table 1). Standard error bars are shown where they are greater than the point. The continuous line was calculated with eqn. (1) using the same method as described for Fig. 6. The interrupted line was calculated using eqn. (2); $\alpha$, $[K]_i$ and $[Na]_i$ were the same as in Fig. 6, and were a constant function of $[K]_o$. $\gamma$ and $[Cl]_i$ were also made a constant function of $[K]_o$ and a series of curves calculated for different $\gamma$ and $[Cl]_i$. The closest approximation to the experimental curve, determined by the least-squares method, is shown with the interrupted line and was calculated with $\gamma = 1$ and $[Cl]_i = 27$ mM (see text).

Fig. 8. Membrane potential, $V_m$ in mV, shown as a function of the logarithm of external K, $[K]_o$ in mM. The filled circles are the average potentials recorded from one red sternomastoid bundle exposed to different concentrations of external K with constant external Cl (160 mM; solutions A and C, Table 1) under isotonic conditions. The continuous line was calculated using eqn. (1) in the same way as for Figs. 6 and 7. The interrupted line through the points was calculated with eqn. (2) as described for Fig. 7. The best fit to the experimental data was obtained when $\alpha = 0{\cdot}008$, $\gamma = 0{\cdot}5$ and $[Cl]_i = 12{\cdot}5$ mM.

with $[K]_o$ = 3·5 mM, $[Na]_o$ = 143 mM and $[Cl]_o$ = 160 mM was −82 mV. The curve calculated with eqn. (1), in the same way as curves for Figs. 6 and 7 (continuous line), does not fit the data. On the other hand the data could be fitted with eqn. (2) when $\gamma$ = 0·5 and $[Cl]_i$ = 12·5 mM or if $\gamma$ was set equal to 4 and $[Cl]_i$ allowed to vary. The best fits were obtained when $[Cl]_i$ increased from 8·0 mM for $[K]_o$ = 3·5 mM, to 68 mM for $[K]_o$ = 75 mM. It is obvious that eqn. (1) could also be made to fit the data in Figs. 7 and 8 by allowing $[K]_i$ to increase with $[K]_o$. However, $[K]_i$ would have to reach concentrations in excess of 300 mM in 150 mM-$[K]_o$ (Fig. 7) or 400 mM in 200 mM-$[K]_o$ (Fig. 8) to fit the data. It is unlikely that $[K]_i$ could increase by this amount without significant swelling and damage to the fibres. As shown above the data can be fitted by eqn. (2) using reasonable values for internal ion concentrations and ion permeability ratios provided the internal and external Cl concentrations are out of equilibrium with $V_m$. Cl redistribution may occur in high $[K]_o$ but this could never be sufficient to allow $V_m = E_{Cl}$.

## DISCUSSION

There is no doubt that Cl ions influence the steady-state membrane potential of fibres from the particular mammalian skeletal muscles used in the experiments described above. The variation of membrane potential with $[Cl]_o$ and with $[K]_o$ can be described in terms of the GHK equation if $[Cl]_i$ is allowed to be out of equilibrium with the steady-state membrane potential. If this is the case, then $[Cl]_i$ must be set by active transport of Cl across the surface membrane. A second possible explanation for the results is that Cl modulates the relative Na and K permeabilities ($\alpha$) and hence indirectly influences the membrane potential. The mechanism for this would have to depend on $[K]_o$ and $[Cl]_o$ in a complex way to fit the data. The direct contribution of Cl movements to the membrane potential is adequate to explain the results and the following discussion is in terms of this hypothesis.

Reports of experiments with rat diaphragm fibres (Palade & Barchi, 1977) and goat intercostal fibres (Bryant & Morales-Aguilera, 1971) suggest that the steady-state membrane potential in these preparations is independent of $[Cl]_o$. These results present an apparent contradiction to the results reported above and so one preparation from a rat diaphragm was examined (see Fig. 2, triangles). The membrane potential was measured 20 min after exposure to low $[Cl]_o$ and in 160 mM-$[Cl]_o$ before and after exposure to each low $[Cl]_o$. Transient potential changes were seen each time $[Cl]_o$ was altered and these were in the same direction as the transient changes described for a EDL, soleus and sternomastoid fibres (see Results). In marked contrast however the membrane potential returned to the same average value for each value of $[Cl]_o$ (see Fig. 2, triangles). It would seem therefore that the internal Cl concentration in the rat diaphragm, and perhaps goat intercostal muscles, is not controlled in the same way as it is in rat *sternomastoid* or mouse *EDL* and *soleus* muscles.

The existence of a Cl 'pump' in some mammalian muscles would not be surprising since energy dependent Cl transport has been suggested in a number of other excitable cells. Mammalian neurones (Lux, 1971; Llinas *et al.* 1974), aplysia neurones (Brown *et al.* 1970), squid giant axons (Keynes, 1963; Scruggs & Landowne, 1975;

Russell, 1976) and giant barnacle muscle fibre (Dipolo, 1972) all demonstrate behaviour consistent with the presence of a Cl pump. Cl permeability is low in these preparations (see e.g. Baker, Hodgkin & Shaw, 1962; Hagiwara, Gruener, Hayashi, Sakata & Grinnell, 1968) and the ion does not significantly influence the resting membrane potential. Cl permeability appears to be high in mammalian muscle and Cl could function in setting the resting membrane potential.

Some predictions on the nature of Cl transport can be made from consideration of the data in Figs. 1, 2 and 3. The direction of Cl transport in 3·5 mM-$[K]_o$ solutions is probably inward as in some aplysia neurones (see e.g. Brown *et al.* 1970) and squid giant axons (Keynes, 1963). The above results suggest that $E_{Cl}$ is more positive than the resting membrane potential of mammalian muscle in 3·5 mM-$[K]_o$. Indeed the progressive hyperpolarization as $[Cl]_o$ was reduced from 160 to 3·5 mM (Fig. 2) implies that $E_{Cl}$ was more positive than $V_m$ at each external Cl concentration. Values of $[Cl]_i$ calculated as described in the legend to Fig. 3 give an $E_{Cl}$ of $-62$ mV in 160 mM-$[Cl]_o$ where $V_m = -74$ mV and an $E_{Cl}$ of $-75$ mV in 35 mM-$[Cl]_o$ where $V_m = -90$ mV. Since there is an outward driving force on Cl in both cases, Cl transport must have been inward to maintain the internal concentration. The reduction of $[Cl]_i$, in low $[Cl]_o$, is consistent with the active-Cl-transport hypothesis if the transport rate depends on $[Cl]_o$ over the range of Cl concentrations used. The rate of ion transport has been shown to depend on ion concentration in several situations including Cl self exchange in red blood cells (Funder & Wieth, 1976) and K influx in frog semitendinosus fibres (Horowicz *et al.* 1968). The significant hyperpolarization with a reduction in external Cl from 160 to 100 mM (Fig. 2) suggests that the transport mechanism is unsaturated or only just saturated at normal external Cl concentrations.

The steady-state distribution of Cl in high $[K]_o$ solutions cannot be determined with certainty from results presented in Figs. 7 and 8. However, as described in the Results section, the recorded membrane potentials can be predicted by the GHK equation for Na, K and Cl, using reasonable values for all parameters, if $[Cl]_i$ is made to increase as $[K]_o$ increases. Additional evidence for Cl redistribution during exposure to high $[K]_o$ comes from the fact that the rate of depolarization caused by high $[K]_o$ is faster in Cl-free solutions as shown in Fig. 5. Cl redistribution must proceed very much more quickly in these preparations than it does in amphibian preparations in similar conditions (Hodgkin & Horowicz, 1959) since the steady-state membrane potential is reached within a few minutes of exposure to the high K solution. Cl conductance in goat intercostal preparations (Lipicky & Bryant, 1966) and in rat diaphragm preparations (Palade & Barchi, 1977) is considerably higher than it is in amphibian skeletal muscle preparations (Gage & Eisenberg, 1969). A similarly high Cl conductance in the mammalian preparations used in the present experiments would account for an increase in the rate of depolarization following Cl redistribution. Whether the observed twelve-fold increase in the rate of depolarization can be accounted for entirely in terms of a higher Cl conductance is questionable.

The author is indebted to Professor P. W. Gage for helpful discussion during the experiments and preparation of the manuscript and to Dr D. Davey for reading the manuscript. I am grateful to Miss M. Dlutowski and Miss B. Mangano for their technical assistance, to Mr G. Williams for photography.

The work was supported by a grant from the Muscular Dystrophy Associations of America.

REFERENCES

BAKER, P. F., HODGKIN, A. L. & SHAW, T. T. (1962). The effects of changes of internal ionic concentrations on the electrical properties of perfused giant axons. *J. Physiol.* **164**, 355–374.

BARRY, P. H. & DIAMOND, J. M. (1970). Junction potentials, electrode standard potentials, and other problems in interpreting electrical properties of membranes. *J. Membrane Biol.* **3**, 93–122.

BOYD, I. A. & MARTIN, A. R. (1959). Membrane constants of mammalian muscle fibres. *J. Physiol.* **147**, 450–457.

BROWN, A. M., WALKER, J. L. & SUTTON, R. B. (1970). Increased chloride conductance as the proximate cause of hydrogen ion concentration effects in Aplysia neurons. *J. gen. Physiol.* **56**, 559–582.

BRYANT, S. H. (1969). Cable properties of external intercostal muscle fibres from myotonic and non myotonic goats. *J. Physiol.* **204**, 539–600.

BRYANT, S. H. & MORALES-AGUILERA, A. (1971). Chloride conductance in normal and myotonic muscle fibres and the action of monocarboxylic aromatic acids. *J. Physiol.* **219**, 367–383.

DIPOLO, R. (1972). Chloride fluxes in isolated dialyzed barnacle muscle fibers. *J. gen. Physiol.* **60**, 471–497.

DULHUNTY, A. F. (1977*a*). K-contractures and membrane potential in mammalian skeletal muscle. *Nature, Lond.* **266**, 75–77.

DULHUNTY, A. F. (1977*b*). Chloride ions and membrane potential in mammalian skeletal muscle fibers. *Proc. Aust. Physiol. Pharmacol.* **8**, 84*P*.

DULHUNTY, A. F. & HOROWICZ, P. (1975). Frog muscle potentials in low external K solutions. *Fedn Proc.* **34**, 467*P*.

EISENBERG, R. S. & GAGE, P. W. (1969). Ionic conductances of the surface and transverse tubular membranes of frog sartorius fibers. *J. gen. Physiol.* **53**, 279–297.

FUNDER, J. & WIETH, J. O. (1976). Chloride transport in human erythrocytes and ghosts: a quantitative comparison. *J. Physiol.* **262**, 679–689.

HAGIWARA, S., GRUENER, R., HAYASHI, H., SAKATA, H. & GRINNELL, A. D. (1968). Effect of external and internal pH changes on K and Cl conductances in the muscle fiber membrane of a giant barnacle. *J. gen. Physiol.* **52**, 773–793.

HODGKIN, A. L. & HOROWICZ, P. (1959). The influence of potassium and chloride ions on the membrane potential of single muscle fibres. *J. Physiol.* **148**, 127–160.

HODGKIN, A. L. & HOROWICZ, P. (1960). The effect of sudden changes in ionic concentrations on the membrane potential of single muscle fibres. *J. Physiol.* **153**, 370–385.

HOROWICZ, P., GAGE, P. W. & EISENBERG, R. S. (1968). The role of the electrochemical gradient in determining potassium fluxes in frog striated muscle. *J. gen. Physiol.* **51**, 193–203.

KEYNES, R. D. (1963). Chloride in the squid giant axon. *J. Physiol.* **169**, 690–705.

LIPICKY, R. J. & BRYANT, S. H. (1966). Sodium, potassium, and chloride fluxes in intercostal muscle from normal goats and goats with hereditary myotonia. *J. gen. Physiol.* **50**, 89–111.

LLINAS, R., BAKER, R. & PRECHT, W. (1974). Blockage of inhibition by ammonium acetate action on chloride pump in cat trochlear motorneurons. *J. Neurophysiol.* **37**, 522–532.

LUFF, A. R. & ATWOOD, H. L. (1972). Membrane properties and contraction of single muscle fibres in the mouse. *Am. J. Physiol.* **222**, 1435–1441.

LUX, H. D. (1971). Ammonium and chloride extrusion: Hyperpolarizing synaptic inhibition in spinal motoneurons. *Science, N.Y.* **173**, 555–557.

PALADE, P. T. & BARCHI, R. I. (1977). Characteristics of chloride conductance in muscle fibres of the rat diaphragm. *J. gen. Physiol.* **69**, 325–342.

RUSSELL, J. M. (1976). ATP-dependent chloride influx into internally dialyzed squid giant axons. *J. Membrane Biol.* **28**, 335–349.

SCRUGGS, V. & LANDOWNE, D. (1975). The temperature dependence of chloride fluxes in the squid giant axon. *Biophys. J.* **15**, 126a.